A Novelty Patching of Circular Random and Ordered Techniques on Retinal Image to Improve CNN U-Net Performance

by Anita Desiani

Submission date: 28-Mar-2023 07:07PM (UTC+0700)
Submission ID: 2048973231
File name: patching_anita.pdf (2.62M)
Word count: 10231
Character count: 51795

A Novelty Patching of Circular Random and Ordered Techniques on Retinal Image to Improve CNN U-Net Performance

Anita Desiani, *Member*, *IAENG*, Erwin, *Member*, *IAENG*, Bambang Suprihatin, Ermatita, Fathur R. Husein, Yogi Wahyudi

***Abstract*— U-Net is one of the CNN architectures with deep layers that requires a lot of training and testing data. Unfortunately, the retinal image data is not freely available. The large images can add parameters and network complexity for U-Net. To improve the ability of U-Net in retinal blood vessels segmentation, it is necessary to provide sufficient with small data size. The blood vessels of the retina are located inside the retina circle. This study proposes a circular random patching and ordered patching technique to cut an image in certain size. The circular random patching uses the Euclidean distance at any point inside the retinal circle. If the patching technique is applied carelessly and does not pay attention to the circle area of the retina, it could cause the outer part of the retina circle that does not contain blood vessels to be taken. This technique proposes to meet the training data requirements of the U-Net architecture by generating as possible many patch images as containing retinal blood vessels. The ordered patching technique is used to obtain the patch images by cutting the entire original image orderly starting from the first pixel point in the image at the testing stage. At final testing stage, the output of patch images has to be reassembled to be reconstructed to its original size with segmented retinal blood vessels features. The proposed method has been implemented on the DRIVE and STARE datasets. The results obtained in DRIVE produced excellent accuracy, specificity sensitivity, F1-score, and IoU. The results in STARE were quite well for accuracy, specificity, and sensitivity, but the F1-score and IoU on STARE are insufficient so that both scores are needed to be improved. The research shows that both the circular random patching in the training stage and ordered patching in the testing stage able to improve the performance of U-Net. The next step for future work is going to combine the proposed patching technique with other CNN architectures to improve the results of retinal blood vessels segmentation performance.**

***Index Terms*— Blood Vessels, Diabetic Retinopathy, Patching, Retina, Retinal Circle, U-Net**

Manuscript received October 1, 2021; revised August 29, 2022.

Anita Desiani is an Assistant Professor of Mathematics Department and Phd candidate of Mathematics and Natural Science Faculty, Universitas Sriwijaya, Indralaya, 30662, Indonesia (e_mail: anita_desiani@unsri.ac.id)

Erwin is an Associate Professor of Computer Engineering Department, Computer Science Faculty, Universitas Sriwijaya, Indralaya, 30662, Indonesia (Corresponding author, phone: 6281394497590, e_mail: erwin@unsri.ac.id).

Bambang Suprihatin is an Associate Professor of Mathematics Department, Mathematics and Natural Science Faculty Universitas Sriwijaya, Indralaya, 30662, Indonesia (e_mail: bambangs@unsri.ac.id).

Ermatita is an Associate Professor of Computer Engineering Department, Computer Science Faculty, Universitas Sriwijaya, Indralaya, 30662, Indonesia (e_mail: ermatita@unsri.ac.id).

Fathur Rachhman Husein is an undergraduate student of Mathematics Department, Mathematics and Natural Science Faculty Universitas Sriwijaya, Indralaya, 30662, Indonesia (e_mail: 08011381621046@unsri.ac.id).

Yogi Wahyudi is an undergraduate student of Mathematics Department, Mathematics and Natural Science Faculty UniversitasSriwijaya, Indralaya, 30662, Indonesia (e_mail: 08011181722009@unsri.ac.id).

I. Introduction

DEEP learning is an artificial neural network method by imitating the work of the nerves of the human brain to process data and learn the pattern of data by computer so that the computer can make decision. Deep learning is one of the neural network which is very popular recently [1]. The classification process that widely uses deep learning has grown rapidly used in various studies [2]. One of the popular methods in deep learning is Convolution Neural Network (CNN). CNN can handle large-dimensional data such as images because input of the CNN should be in the matrix form [3]–[6]. One of the most widely used in CNN architectures for segmentation in medical image analysis is U-Net [7]. U-Net provides a good performance for segmentation feature and classification of diagnoses on medical images [3], [8], [9].

Several studies have applied U-Net for image segmentation. Ronneberger et al. [7] applied U-Net architecture for medical image segmentation, Soomro et al. [10] modified U-Net architecture with Variational-Auto-Encoder (VAE) on retinal blood vessels segmentation, and Li et al. [11] modified U-Net as a new architecture named Iter-Net for retinal blood vessels segmentation. Others study using U-Net were Yan et al. [12] on Digital Retinal Image for Vessel Extraction (DRIVE) and Structured Analysis of the Retina (STARE) datasets, and Jin et al. [13] did combination between deformable and U-Net on the DRIVE dataset. Unfortunately, these studies still yield a sensitivity below 77%. U-Net architecture has several layers that are deep enough [14]. Adding layers directly to the U-Net network can increase the parameters and complexity of the network. This can lead to vanishing gradient problems and excessive complexity during training [15], especially for large size of images. Image datasets are available in various datasets on internet such as DRIVE, STARE, CHASE-DB, etc. The datasets have large size of images but they are less quantity. According to Hamwood et al. [16], the performance of U-Net is influenced by the amount of training data used and the size of the image applied. In addition, the large size of image affects the training process. The larger the image size, the more memory is required. However, a less amount of training data can lead to decrease the performance for machine learning in exploring features. To handle this

problem, we can do by using certain techniques to generate training data. One of the techniques has been widely used is patching technique. Patching is a technique that works to divide an image into small pieces of image. This technique is usually used to retrieve certain features or reproduce training data [17]. The patching technique divides the image into multiple images with the same size [15], [18], [19]. If patching process is done carelessly then the unused features will be also detected during the training process. The patching technique on retinal image blood vessels requires a certain approach technique. A combination of patching technique and U-Net architecture is an alternative idea to increase the amount of data and U-Net performance on training stage.

The retinal blood vessels are inside the retinal circle or the eyeball. If the patching technique only divides the image within a certain size, then part of the image that does not contain blood vessels is captured. In addition, the size of different patching also affects the convolution operation on encode and decode of U-Net. The convolution operation of U-Net has $2^n x 2^n$ size of the feature map so the image patch should have $2^n x 2^n$ size of image. The other problem, if the patching technique divides the image into a certain size, then the number of patches obtained is sometimes not sufficient for amount of training data needed. The training stage is very important in recognizing patterns for label data. The success of an algorithm in training stage is very important in determining the performance of an algorithm or method in testing stage. U-Net in training stage requires a huge amount of training data. Currently, the availability of retinal blood vessels image data is still very limited. To handle the limited amount of data, special patching technique is required. The patching technique should be able to generate as much as possible images patch so meet the required amount of data, especially at the training stage. The patching technique on retinal images requires a certain approach because the blood vessels taken are only in the retinal circle so the area available for taking blood vessels on retinal images is limited. This study uses circular random patching. The patching detects the features that were in a retinal circle using Euclidean distance. In contrast to patching at the testing stage, the patching technique does not focus on getting the features of blood vessels. In testing stage, the weights obtained in training stage are be applied to image data test to get retinal blood vessels. The patched images have to be rearranged easily become original size of image. The resulting images in testing stage are not like the original image but the images with segmented retinal blood vessels as in original size of image. In the testing stage, the proposed patching technique is to divide the image into several patches with equal size. Training state results weights that should be applied into patch images in testing stage. This patching is necessary to facilitate the reconstruction process to obtain segmented image. This technique namely as the ordered patching technique. The combination of the circular random patching technique at the training stage and the ordered patching technique at the testing stage expects to be able to improve performance on the U-Net architecture. The combination on proposed method would be an alternative method to improve training data and increase the performance of U-Net architecture for retinal blood vessels segmentation. The better the performance of the U-Net architecture, the more accurate as well as valid the retinal blood vessels segmentation results will be.

II. Related Work

Several modification of U-Net architecture have been renewed for various data purposes. Trebing et al. [20] used Small Attention-U-Net model, where the encoder part was modified by adding a convolution block, which was taking the input image in a series placed on double convolution, while the decoder section was modified with Bilinear Up-sampling. The result of this study on precipitation map dataset produced an accuracy of 82.9%, specificity of 73%, sensitivity of 85%, and F1-score of 78.6%. While the study on the cloud cover dataset produced an accuracy of 88.9%, sensitivity of 92.1%, and F1-score of 90.6%. Unfortunately, the average performance results in both datasets was still below the result of conventional U-Net architecture. Rundo et al. [21] used the USE-Net model, which combined the Squeeze-and-Excitation block into the U-Net. Hereafter the USE-Net as compared with three other architectures, namely, U-Net, pix2pix, and Mixed Scale Dense Network. Unfortunately, this study did not calculate other model performance measures such as accuracy, sensitivity, specificity, F1-score, and IoU. Samuel and Veeramalai [22] used the VGG-16 Architecture and vessels-extraction layer on U-Net architecture, where each vessel-extraction layer consists of VSC blocks, SC layers, and feature maps. The performance results for specificity, accuracy, and AUC values in the DRIVE, STARE, and DCA1 datasets were very good above 90% even though the sensitivity was still around 78%. The number of parameters used in the VSSC-Net model were 8 million. Sambyal et al. [23] has modified the U-Net on the encoder section using Residual Networks (ResNets) architecture, on the bridge using middle convolution, and on the decoder section using 4 U-Net blocks for microaneurysm segmentation on the IDRiD dataset. The study produced excellent results of sensitivity, specificity, accuracy, and F1-score values, which are above 90% as well as in the E-optha-MA+IDRid dataset. The segmentation in both datasets also produced excellent results, which are above 90%. The feature segmentations carried out in this study are only on microaneurysms and exudates not on retinal blood vessels. Shehab et al. [24] implemented ResNets-50 architecture by adding a skip connection shortcut on U-Net layers for brain tumor image segmentation. The performance results of this method using the 2015 BRATS dataset had excellent accuracy, specificity, precision, and F1-score values, which are above 85%. However, the method was not used for retinal image. Kose et al. [25] has implemented a Multiscale Encoder-Decoder Network (MED-Net) which consists several encoder-decoder subnets where the basic unit of the sub network consists residual blocks (convolution layer, ReLU, and batch normalization). The MED-Net focused on confocal segmentation of melanocytic lesions image. The results of F1-score and sensitivity were still low only 74% and 77% respectively, while for specificity it is great, of 92%.

In image segmentation, the patching technique is applied to improve features and crop or cut the image as desired. Nortje et al. [19] applied a patching technique by converting the image into a binary form and continued by cutting the image into the same size. Takahashi et al. [26] performed patching to cut and extract important features from multiple images and merge these patches into a new image. The size of the new image was the same as those of the original image. Zhang et al. [18] used a patching technique to improve image quality by cutting all parts of the image into the same size,

fixing the features in each section and reassembling them into their original size. Guo et al. [27] used the KD-forest patching by cutting the image into the same size, and the results of similar patches were combined into a new image.

Hsieh and Shao [28] did patching with a certain size on the blurred image area. The contrast quality of the image patch was enhanced to make image looks clearer. Yu et al. [29] did patching by choosing a size randomly to reduce the dimensions of the image and only the image patch that contained the features needed were taken. Marín et al. [30] performed a patching technique to reproduce new image data with the same size. The patching was did by dividing the entire area of the original image such that the image area does not contain features would be taken. Liu and Yeoh [31] used a patching technique by using different sizes in the image, i.e. 32x32, 64x64, and 16x16 specifically in the image area that contains features of building crack dataset. Tang et al. [32] performed a patching technique by finding similarities between pixel points using the fuzzy k-means method. The patch images were obtained on different sizes. Shi et al. [33] did patching based on the proximity of Euclid's distance. Xiao et al. [34] applied the patching technique by augmenting data. Each data should be extracted 500 times into several patches so that the number of training images is enlarged with a patch size of 64x64. This study used the weighted Res-U-Net architecture for retinal blood vessels segmentation. This architecture was similar to the U-Net architecture but by adding Weighted Attention and skip connection on the Res-Net architecture. The sensitivity produced in this study was still low below 78%.

III. Methodology

A. Retinal Image Dataset

Retinal datasets are widely available and can be accessed free of charge on the internet including the Digital Retinal Images for Vessel Extraction (DRIVE) and Structured Analysis of the Retina (STARE) datasets. DRIVE provides retinal data that can be accessed and obtained on the website https://www.isi.uu.nl/Research/Databases/DRIVE/. DRIVE dataset is a publication of the Image Sciences Institute (ISI) of the Utrecht University. DRIVE dataset comes form observations of 400 diabetic patients. The observation produces 40 images of retinal blood vessels which are divided into two groups, one group had 20 images for training stage known as ground truth and the another group had 20 images for testing stage. All images in DRIVE dataset are also splited into two categories. The first is known as normal class as many as 33 images and secondly is known as mild DR class as many as 7 images. Another dataset is STARE taken from https://cecas.clemson.edu/~ahoover/STARE/ which has been a research project started in 1975 at the University of California. This dataset consists of 400 retinal images. There are 13 disease classes for each retinal image sample in the dataset, including Hollenhorst Emboli, Branch Retinal Artery Occlusion, Cilio-Retinal Artery Occlusion, Branch Retinal Vein Occlusion, Central Retinal Vein Occlusion, HemiCentral Retinal Vein Occlusion, Background Diabetic Retinopathy, Proliferative Diabetic Retinopathy, Coat's, Arteriosclerotic Retinopathy, Hypertensive Retinopathy, Macroaneurism, and Choroidal Neovascularization.

B. Method

The steps used for the proposed method are:

Image Quality Enhancement

The image quality of enhancement process is useful for segmentation process to get the required features. There are three steps of image quality enhancement starting with Grayscale. The next step is to increase the contrast of the image using Gamma Correction and Contrast Limited Adaptive Histogram Equalization (CLAHE). The last is noise reduction and image smoothing using Median Filter and Gaussian Filter.

Circular Random Patching Technique

The STARE has only 20 images for training data while on the DRIVE dataset has 40 images for training data. With less amount of image data, the model would have difficulty to learn the important features. Image with small size but with large amount of image data helps U-Net architecture in studying the multiple retina blood vessel patterns in detail. The patching technique is done to produce more small size training data by partitioning or dividing a large image into smaller subsections.

The circular patching technique works by taking points randomly on retinal image. Fig 1 is an illustration of the circular random patching technique that is carried out in the training stage.

1) Determine the weight (w_s) and the height (h_s) size of patched image, where $h_s = w_s = t$, so the patched image size is $t \times t$, where t is less then weight (w) and height (h) of original image size.
2) Determine the diameter (d), radius (r), and center point of circle (O) at coordinates (x_0, y_0) using Equations (1) and (2),

$$r = \frac{1}{2}(d), \tag{1}$$

$$O(x_0, y_0) = \left(\frac{w}{2}, \frac{h}{2}\right) \tag{2}$$

3) Generate any point $P(x_i, y_i)$ as the midpoint of the patch and calculate the Euclidean distance R between $P(x_i, y_i)$ and $O(x_0, y_0)$ with Eq (3). If the Euclidian distance R is smaller than the length of the radius r $(R < r)$ than then take a patch of r' in square with center point $P(x_i, y_i)$.

$$R = \sqrt{(x_i - x_0)^2 + (y_i - y_0)^2} \tag{3}$$

4) Do patching technique around the point $P(x_i, y_i)$.

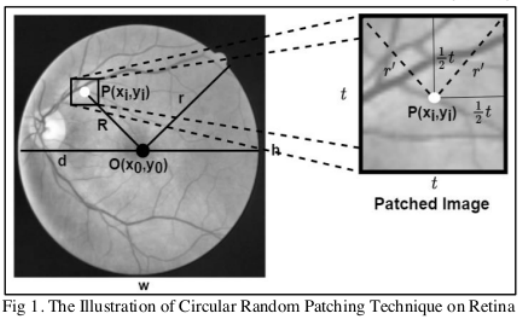

Fig 1. The Illustration of Circular Random Patching Technique on Retina Image

Point $P(x_i, y_i)$ would be the new center point to take another point with a distance (r') on each diagonal axis. The (r') is calculated with Eq (4). The results by taking these points form a new image in the square form.

$$r' = \frac{1}{2} t\sqrt{2} \tag{4}$$

5) Rapid all steps to get the desired training data.

U-Net Architecture

At the training stage, the U-Net architecture is used to find out the features that exist in image data, which is resulted from the image enhancement stage. The U-Net steps used are:

1) Initialize the parameters for number of epochs and batch size.
2) Train the input data which resulted from image enhancement using the U-Net architecture by Equations (5), (6), (7), and (8) as follows [37]:

$$C_q^p = O_q^p + b_q \tag{5}$$

$$O_q^p = A_p * K_q \tag{6}$$

$$o_{x,y} = \sum_{u=0}^{n-1}\sum_{v=0}^{n-1} a_{u+x,v+y} \times k_{x+1,y+1} \tag{7}$$

$$c_{x,y} = o_{x,y} + b_q \tag{8}$$

where $*$ is the convolution operation, x is the row $(x = 1,2,...,n)$, y is the column $(y = 1,2,...,n)$, n is the kernel height and A_p is the p^{th} input matrix, k_q is the q^{th} kernel matrix, b_q is the q^{th} kernel bias, O_q^p is the kernel convolution operation matrix starts from the q^{th} input to the p^{th}, C_q^p is the convolution matrix of the q^{th} kernel input to the p^{th}.

3) Perform the calculation process with the ReLU activation function using Equation (9) [38].

$$a(z) = \max(z,0) \begin{cases} z; z \geq 0 \\ 0; z < 0 \end{cases} \tag{9}$$

Where z is the input to the activation function and $a(z)$ is the result of the ReLU activation function.

4) Reduce the dimensions of feature maps using max pooling.
5) Increase the dimensions of the image features using transposed convolution.
6) Perform the convolutional operation with kernel size of 1×1 and use the sigmoid activation function in Equation (10) [39].

$$\sigma(z) = \frac{1}{1 + e^{-z}} \tag{10}$$

Where $\sigma(z) \in (0,1)$, and $z \in (-\infty, \infty)$.

7) Calculate the loss function using the Binary Cross Entropy formula in Equation (11) [40]:

$$l = -\frac{1}{m \times n}\left(\sum_{i=1}^{m}\sum_{j=1}^{n}\left(y_{ij}\log(p_{ij})\right) + \left(1 - y_{ij}\right)\left(1 - \log(p_{ij})\right)\right) \tag{11}$$

Where $m \times n$ is the size of the matrix, y_{ij} is the entry of the ground truth label matrix, i^{th} of row, j^{th} of column, p_{ij} is the matrix entry predicted by i^{th} of row, j^{th} of column, l is the binary cross entropy error or loss function.

Ordered Patching Technique

Patching technique on testing stage is different with the patching on training stage. In testing stage, patching is done sequentially and divided into the same size for the entire image area. The image patches from this technique will be segmented using the weights obtained in training stage. After that, the patch images will be reconstructed back to its original size that contain of retinal blood vessels. The illustration of the steps that performed on patching ordered can be seen in Fig 2. The steps for ordered patching in the testing are as follows:

1) Determine height w_s and patching width h_s of the patched image where w_s and h_s should be same size $w_s = h_s = t$ and smaller than the original image's width $(w_s \langle w)$ and height $(h_s \langle h)$ so that the patched image size is $t \times t$. Specify the stride s value to be used

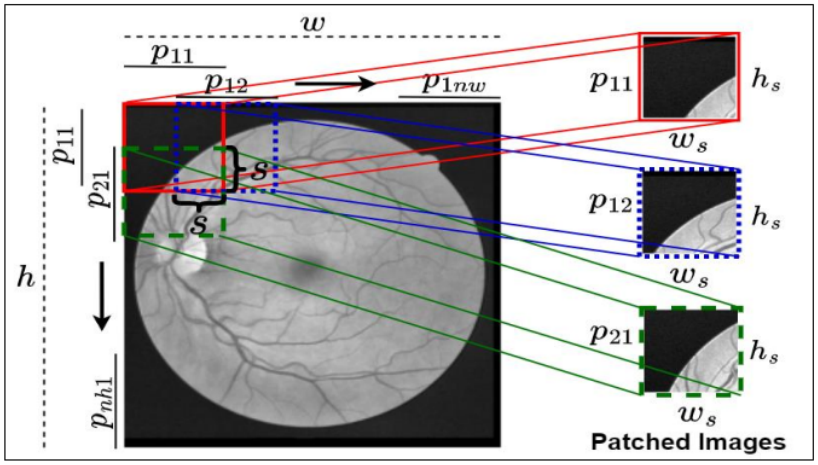

Fig 2. The Ordererd Patching Technique Illustration on The Testing Stage

for shifting from one patched image to another. The value of the variables h_s , w_s and stride s must fulfill Equations (12) and (13).

$$w_s \mid (w-s) = 0 \tag{12}$$

$$h_s \mid (h-s) = 0 \tag{13}$$

This condition is needed in this patching so that during the retrieval process, patch retrieval does not come out from area of original image.

2) Calculate the number of patches (n_w) performed on the width $(w)$of the original image and calculate the number of patches (n_h) performed on the height (h) of the original image with Equations (14) dan (15).

$$n_w = floordiv\left(\frac{(w-w_s)}{s}\right)+1 \tag{14}$$

$$n_h = floordiv\left(\frac{(h-h_s)}{s}\right)+1 \tag{15}$$

3) Take patched images sequentially starting from the first coordinate. The patching technique works according to the predetermined patched image size $h_s \times w_s$.

4) Shift as many as s strides along the width W of the original image starting from row $i=0$ and column $j=0$ to $j=n_w$.

5) Continue by shifting the next line down with $i=1$ and $j=0$ until $j=n_h$. do it on the next patched image until all the coordinates have been patched.

Patched Images Reconstruction

After generating the patched images used the ordered patching technique, the next process is segmentation. In the segmentation process, the weights obtained at the training stage are applied to the patched images. The segmentation results are binary patch images that contain only retinal blood vessels (white) and background (black). These results will be reconstructed to put back the patch images together into a single image with the original size. The flow steps for reconstructing the patched images from the testing stage can be seen in Fig 3. Fig 3 provides an example of 3 patched insertion on the width of the image and the height of the image.

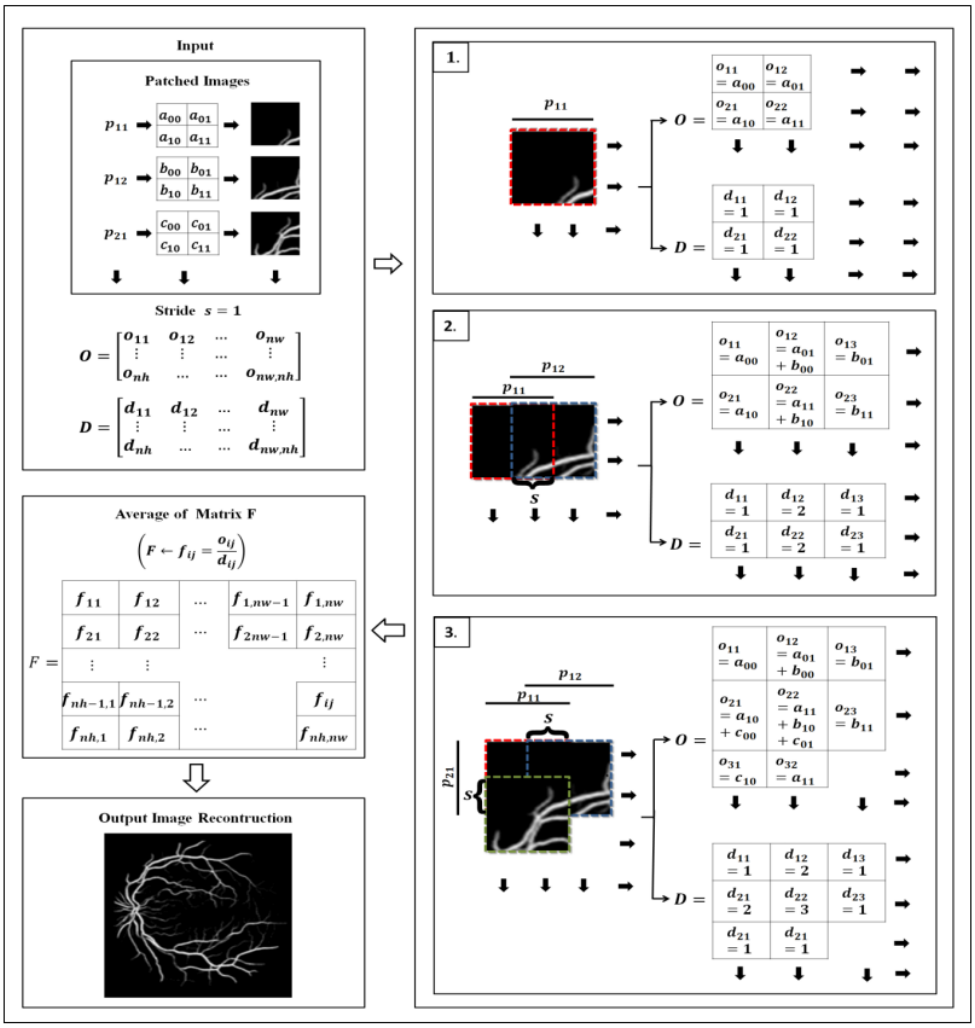

Fig 3. The Reconstruction Result of Patched Images as One Output Image

The steps in reconstructing the segmented patch images are:

1) Prepare a zero matrix O as a place to combine the patched images, and a zero matrix D as a temporary matrix to calculate the addition of each pixel of the patched image to the O matrix. The dimensions of the D and O matrix must be the same as the original matrix sizes of the image before patching.
2) Determine the value of stride s for the distance shift from one patch to another in the matrix O.
3) Insert the patched images into the matrix O according to the order of the patched images in the ordered patching technique. Each time a patched image is entered into the matrix O, the entry o_{ij} in the matrix O will increase by added the value of the pixels in patched image.
4) Shift the position of o_{ij} on the matrix O by stride s so position i will change by a distance of $i+s$ and position j will change by a distance of $j+s$ for the next patched image insertion.
5) Add one to entry d_{ij} $(d_{ij}+1)$ in matrix D if there is a change in the value of entry o_{ij} in matrix O. If the value of entry in matrix O is already filled in, then add up the existing values in the entry with the new value from the patched image to be inserted, and add those changes to the entry in matrix D.
6) Repeat the steps until all patches in the testing stage have been inserted into the O matrix.
7) Perform the operation of dividing all entries o_{ij} in the matrix O by the entries d_{ij} in the matrix D with Equation (10). Put the results in entries f_{ij} in Matrix F.

$$f_{ij} = \frac{o_{ij}}{d_{ij}}, f_{ij} \in F \tag{10}$$

Where o_{ij} is entry in matrix O, d_{ij} is entry in matrix D, $i = 1,2,\cdots,n_w$ and $j = 1,2,\cdots,n_h$.

Performance Evaluation

The performance of the proposed method is evaluated by measures that commonly used in machine learning, namely accuracy (Acc), sensitivity (Sn), specificity (Spe), IoU, and F1-score (F1) obtained at the testing stage [41], [42]. At this step, the results obtained on the proposed method would be compared with the results of other similar studies. All steps carried out on the proposed method could be seen as a flowchart in Fig 4.

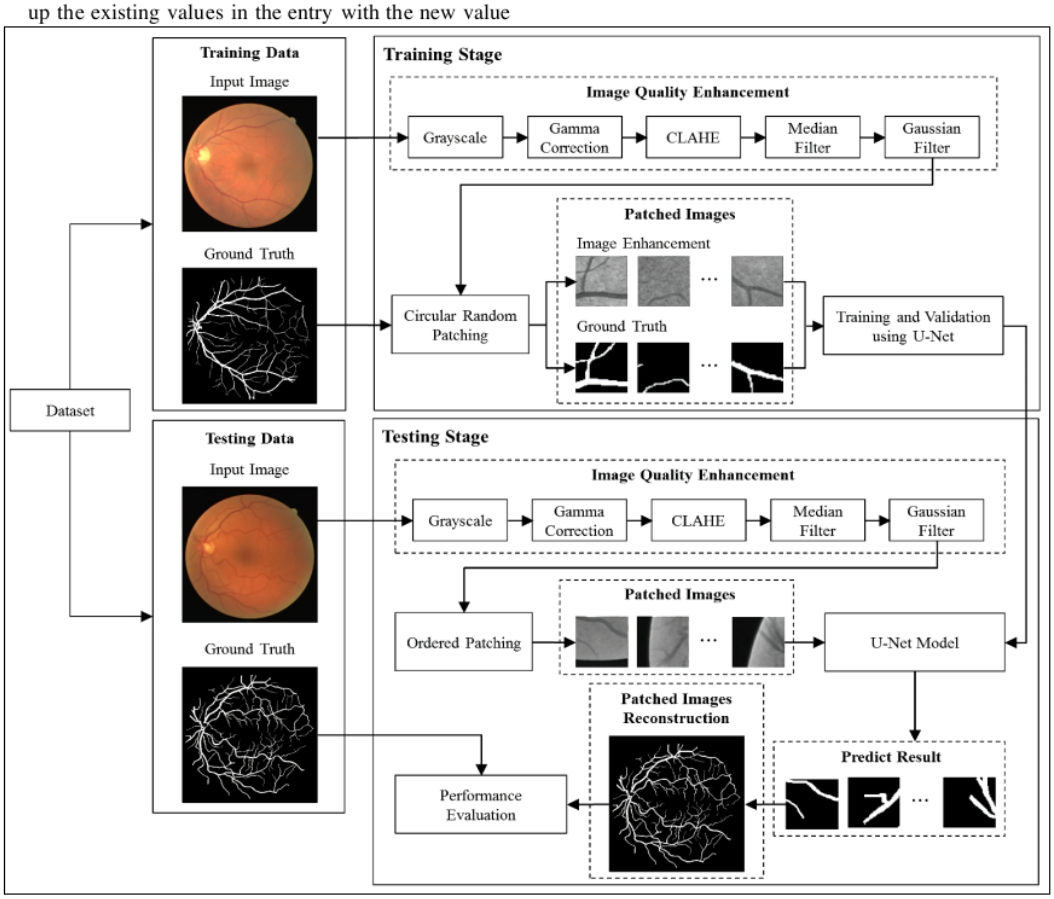

Fig 4. All Steps of Combination Patching Technique and CNN U-Net on Proposed Method

IV. Result and Discussion

After going through the image enhancement process, the obtained image would be patched according to the steps in the proposed method. This circular random patching technique is used to obtain the blood vessels inside the retina circle. Table I is an example of applying circular random patching technique with 40 iterations. In Table I it can be seen that from the initial 40 iterations carried out on the file "21_training.ppm". Only 32 patches can be taken at random points $P(x_i, y_i)$, while for the rest, the patches can not be taken because the Euclidian distance R is larger than the radius r of the retinal circle.

TABLE I
EXAMPLE OF 40 ITERATIONS OF CIRICULAR RANDOM PATCHING ON "21_TRAINING"IMAGE ON DRIVE DATASET

Iteration	x_i	y_i	R	r-r'	$R<r$-r'
1	183	380	139.31	230,06	True
2	325	216	78.92	230,06	True
3	273	260	24.42	230,06	True
4	345	293	63.38	230,06	True
5	446	148	211.71	230,06	True
6	383	289	100.71	230,06	True
7	283	277	5.52	230,06	True
8	524	139	280.92	230,06	False
9	309	167	118.50	230,06	True
10	410	438	201.09	230,06	True
11	452	319	173.39	230,06	True
12	248	275	35.31	230,06	True
13	406	249	127.96	230,06	True
14	168	298	115.54	230,06	True
15	101	311	183.72	230,06	True
16	412	471	228.70	230,06	True
17	448	415	212.01	230,06	True
18	119	513	282.60	230,06	False
19	313	366	88.90	230,06	True
20	529	227	252.67	230,06	False
21	477	309	196.30	230,06	True
22	102	221	190.69	230,06	True
23	199	231	98.10	230,06	True
24	173	153	169.59	230,06	True
25	146	113	217.63	230,06	True
26	59	228	230.05	230,06	True
27	453	159	210.53	230,06	True
28	74	418	248.66	230,06	False
29	334	399	127.38	230,06	True
30	341	400	131.26	230,06	True
31	493	365	226.09	230,06	True
32	70	469	282.73	230,06	False
33	339	53	236.35	230,06	True
34	473	65	289.13	230,06	False
35	277	465	182.58	230,06	True
36	368	32	264.69	230,06	False
37	328	272	46.70	230,06	True
38	291	120	162.72	230,06	True
39	257	232	56.57	230,06	True
40	150	492	247.88	230,06	False

In Table I it can be seen that there are 40 initial iterations carried out on the "21_training.ppm" image using circular random patching technique. The experiment results 32 patched images that can be retrieved at points $P(x_i, y_i)$. Meanwhile, the rest patched images are not be taken because they are outside the retinal circle. The Fig 5 shows the results of the circular random patching technique on the "21_training.ppm" data DRIVE based on the calculations as in Table I.

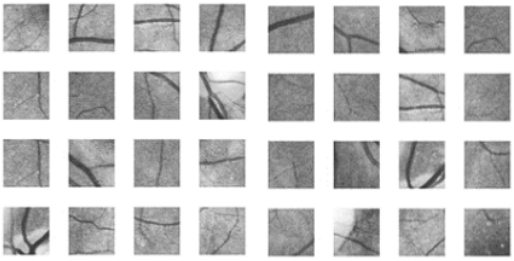

Fig 5. The Result of 32 Patch Images from Circular Random Patching by Generating 40 Random Points

A. Segmentation

Image segmentation is to separate a crucial part from other parts on retinal image. The crucial part is known as foreground and the others known as background [43]. Segmentation is the process of separating the used and not used feature. The results of the patching process of the example in Fig 5 become the input for the segmentation process. At segmentation, the data is divided into training data and testing data. The CNN architecture used for segmentation is the U-Net architecture. Fig 6 shows the process in the U-Net architecture. The patching size for the image used on the proposed method is 48×48, which is considered enough size for this architecture. The segmentation is divided into 2 stages, namely the training and testing stages where each stage has a different patching technique.

B. Training

In the training stage, the training process is carried out using the CNN U-Net Architecture which is illustrated in Fig 6. The steps in the U-Net architecture consist of two paths, namely the Encode path and the Decode path. In the encode path, the convolution block process is resulted by Equation (1) with 32 filters and used the same padding on the 1st convolution block. After the first convolution with 32 filters, 20% of the feature map is set to zero (0) with a dropout screen. After passing the dropout screen, 32 feature maps would be convoluted again as with the previous convolution block process. After that, the dimension of feature maps is reduced using the max pooling in Equation (2). The same process is performed on the encode path for the 2nd, 3rd, and 4th convolution blocks with the number of filters in a row, namely 64, 128, and 256.

The next step is the convolution process in the 5th convolutional block using the ReLU activation function (Equation (3)) but it does not use max pooling in the connecting line with some filters of as many as 512. In the decode path, the transposed convolution process is carried out with some filters as many as 256 in the 6th convolutional block. The next stage is to combine the results of the transposed convolution in the 6th convolutional block in the decoding path with the convolutional results in the 4th convolutional block in the encode path. The result of this combination is convoluted with the 256 number of filters like the previous convolution block process. The same process is

carried out on the decode path for the 7th, 8th, and 9th convolutional blocks with the number of filters, namely 128, 64, and 32, respectively. The convolution block process is performed again using the convolution size of 1x1 and applied with the sigmoid activation function.

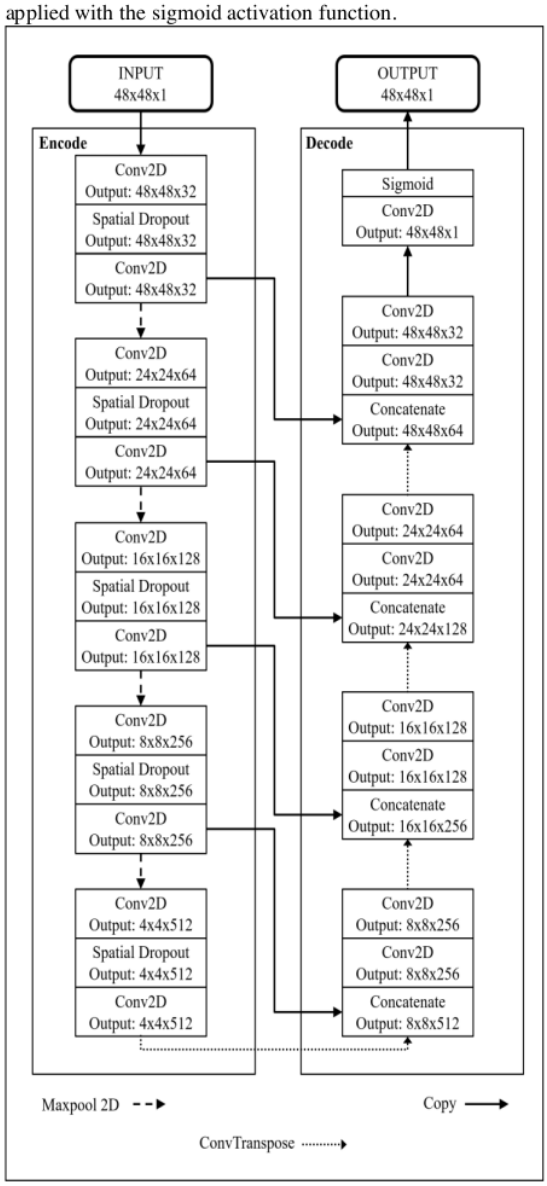

Fig 6. CNN U-Net Architecture with Input Size of 48x48 for Each Circular Random Patched Image

The training process using the CNN U-Net architecture is applied to the DRIVE and STARE datasets. The results of the training process for the DRIVE dataset and the STARE dataset per epoch appear the growth of accuracy score (Fig 7). The increase in accuracy for DRIVE and STARE datasets shows that the proposed method has a good learning to detect blood vessels on the retinal image. In each epoch, the accuracy results always increase and does not change when entering the 30th epoch and so on. Even though the final accuracy of the STARE dataset is higher than the DRIVE dataset, the training accuracy of the DRIVE dataset is more stable, it can be seen that the accuracy always increased with the addition of each epoch. This indicated that the model implemented in the training process for both datasets has been running well. The next stage is the best weights in the training process would be saved in the model and used in the testing process. The combination of U-Net CNN and Circular Random Patching technique at the training stage produces 7 million parameters with a patch image size of 48x48. The average execution time per image in the proposed method is around 20 seconds for the DRIVE dataset and 23 seconds for the STARE dataset.

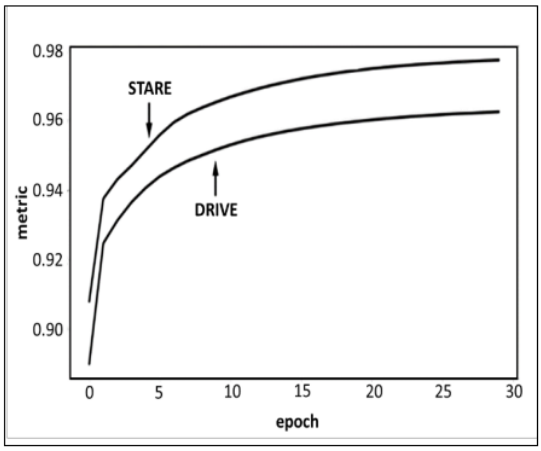

Fig 7. Training Accuracy Results per Epoch on The DRIVE and STARE Dataset

C. Testing

At the testing stage, the steps taken to test the model are to use new data that has not been used in training. This is given to test whether the resulting model has been applied and can retrieve the information that has been learned during the training process. In the testing process, the sequential patching technique is carried out by dividing the original image directly with the same size, and the patching technique is carried out sequentially from right to left of the image and continued to the bottom according to the desired patching size. After that, the weights obtained in the training process are applied to the patched image to segment the existing blood vessels in each sequenced patching image.

The results of the tests are carried out on the DRIVE and STARE datasets using the test data provided in the datasets. The result of segmentation is a patched image that has succeeded in recognizing retinal blood vessels. The segmentation results from each patched image are reconstructed back to their original size with the resultant segmented veins. Table II is a comparison between the segmentation results obtained with the results on the ground truth provided by the dataset. Before the comparison is made between the reconstruction process, the same thing is done, namely combining the segmentation results from each segmented patch image and calculating the average pixel value which is the intersection of one patched image with another patched image. The reconstruction process is the opposite of the patching process, which is rearranging the patched image back to its original image size.

TABLE II
COMPARISON OF GROUND TRUTH WITH SEGMENTATION TEST RESULTS USING CIRCULAR RANDOM PATCHING TECHNIQUE AND U-NET ARCHITECTURE ON DRIVE AND STARE DATASETS

STARE			DRIVE		
Original	Ground Truth	Prediction	Original	Ground Truth	Prediction
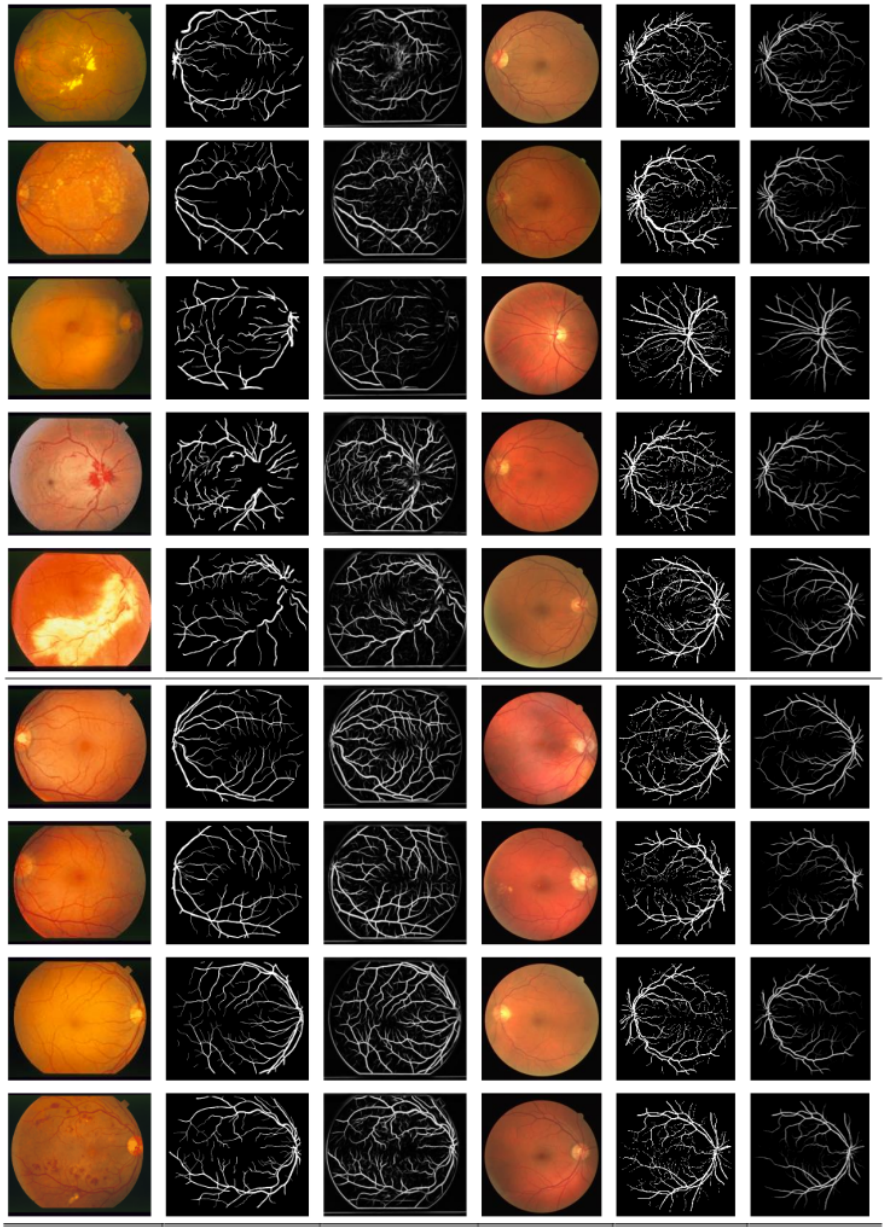					

In Table II, retinal blood vessels segmentation from testing are quite similar to the ground truth provided in the DRIVE and STARE datasets. In Table II the thin branch of the blood vessels can be seen clearly in the segmented image according to the ground truth. To measure the performance of the proposed method, a confusion matrix iss used to measure accuracy, sensitivity, specificity, F1-score and IoU. The results of the confusion matrix can be seen in Table III.

From the confusion matrix in Table III, the performance of the proposed method on the DRIVE and STARE datasets can be measured. For the DRIVE dataset, the results obtained were as follows, accuracy was 98.73%, sensitivity is 85.35%, specificity is 100%, F1-score was 92.09% and IoU is 85.35%. In the STARE dataset, the accuracy value is 93.08%, specificity is 93.65%, sensitivity is 86.2%, F1-score and IoU obtained are 65.26% and 48.3%, respectively.

TABLE III
RESULTS OF CONFUSION MATRIX ON RETINAL IMAGE BLOOD VESSELS SEGMENTATION USING CIRCULAR RANDOM PATCH TECHNIQUE, U-NET, AND ORDERED PATCHING ON DRIVE AND STARE

Segmentation Result	*Ground truth*			
	DRIVE		STARE	
	Blood Vessels	Background	Blood Vessels	Background
Blood Vessels	493282	84663	555165	88888
Background	0	6101735	502173	7402254

From the results of the confusion matrix calculation results in Table III, it can be seen that the F1-score and IoU values in the STARE dataset were still low (under 70%). It indicates that the model by U-Net architecture's ability to separate the foreground (retinal blood vessels) and background (other features) areas still needs to be improved. This is in contrast to the results shown in the DRIVE dataset. The confusion matrix in Table III for the DRIVE dataset gives a very good and excellent performance. The results where the value of each performance measure of the proposed method has given results above 85%. The number of retinal and background blood vessel pixels in the DRIVE and STARE datasets is not balanced. From Table III, it can be seen that the number of background pixels is more than the number of blood vessel pixels. To measure the performance of the model on unbalanced data, the Matthews correlation coefficient (MCC) is used. The MCC value obtained in the DRIVE dataset is 0.92, while for the STARE dataset the MCC value obtained is 0.64. The MCC values in both datasets are almost close to 1. These results indicated that the proposed method is able to work well even though the number of classes in the data was not balanced. In addition, the ROC evaluation on both datasets is used to measure the results of the proposed method on both the DRIVE and STARE datasets.

Fig 8 shows the results of ROC and AUC in the two datasets used. This is to determine the increase in ROC and the area of the AUC obtained. Fig 8 shows that the area under the ROC curve graph obtained is equal to or close to 1, especially in the performance results on the DRIVE dataset. In the DRIVE dataset, the number of True Positives obtained was greater than the number of False Positives. On the other hand, in the STARE data, although the ROC curve s also close to one, its value is still below the result in the DRIVE dataset. This is influenced by a significant False Positive rate. From Fig 8, it can be seen that the AUC curve area is very good for both datasets. The AUC in the DRIVE data has a perfect value of 1 and the AUC in the STARE data is close to 1, which was 0.9607. This shows that the segmentation results carried out by the model on retinal blood vessels can provide good quality.

In this study, the segmentation process has been carried out using a combination of circular random patching technique, CNN U-Net, and ordered random patching technique. To see the extent to which the success of the proposed method, the performance results of this study are compared with several other studies related to blood vessels segmentation. The comparison between the results obtained in other studies and in the proposed method is shown in the Table IV for DRIVE dataset and Table V for STARE dataset.

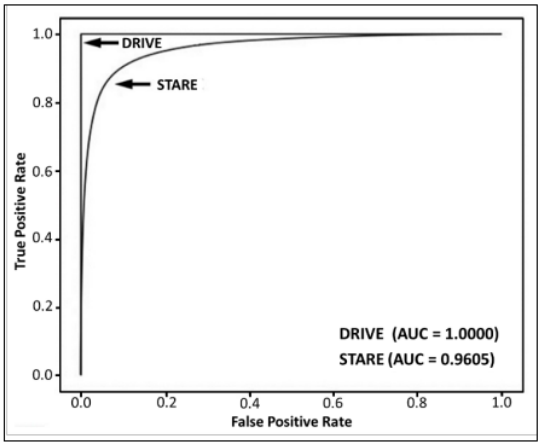

Fig 8. ROC with Curve Area (AUC) Test Results on The Proposed Method for DRIVE and STARE Datasets

TABLE IV
RESULTS COMPARISON OF THE PROPOSED METHOD WITH OTHER STUDIES FOR DRIVE DATASET

Method	Acc (%)	Sn (%)	Spe (%)	IoU (%)	F1 (%)
SA-U-Net [45]	96.98	82.12	98.4	-	82.63
Strided U-Net [10]	95.9	80.2	97.4	-	-
M-GAN [42]	97,06	83,46	98.36	71,29	83,24
MRU-Net [46]	96,11	86,18	-	72,91	84,44
U-Net Shrinking path [47]	94,7	70.92	98.2	-	-
MDCF-I+U-Net [48]	-	83,14	81,57		82,35
DU-Net [13]	95.66	79.63		82.37	
Patch-based Generative Adversarial Network [49]	95,62	98,24	77,46	-	-
U-Net [50]	95.54	78.49	98.02	-	81.75
PixelBNN[51]	92.2	73.5	98.3	-	76.5
MRA-Net[52]	96.9	83.5	98.2		82.9
Proposed Method	98,37	85,4	100	85,4	92,07

Table IV presents a results comparison of the proposed method on the DRIVE dataset with other similar studies. The application of the circular random patching technique and CNN U-Net architecture in the DRIVE dataset has given excellent results. The performance results from testing on DRIVE are superior to STARE results. In table IV, it can be seen that the proposed method has the best results compared to other studies for accuracy, specificity, IoU, and F1-score. Although the highest sensitivity is obtained by Abbas et al. [49] but their specificity was still below 80%. It illustrated that their study has not been maximized to segment background. In addition, the study did not measure the F1-score and IoU. Research by Park, Choi, and Lee [42] and Ding et al. [46] also measured their performance using IoU and F1-score, but those were still lower than IoU and F1-score on the proposed method. The F1-score on the proposed method is 85.4%. It indicated that the proposed method had a very good balance in the blood vessels segmentation or the background segmentation. The IoU on the proposed method is the highest compared to other studies. This shows that the proposed model is great at distinguishing the region between blood vessels as foreground and other

regions as the background correctly.

TABLE V
RESULTS COMPARISON OF THE PROPOSED METHOD WITH OTHER STUDIES FOR STARE DATASET

Method	Acc (%)	Sn (%)	Spe (%)	IoU (%)	F1 (%)
H-DenseU-Net [53]	96.51	68.07	99.16	-	76.91
Strided U-Net [10]	96.1	80.1	96.9	-	81.27
U-Net [50]	96.37	76.4	98.65	-	-
M-GAN [42]	98.76	83.24	99.38	71.98	83.70
MRU-Net [46]	96.62	78.87	-	68.64	81.43
MDCF-I+U-Net [48]	-	79.24	98.27	-	-
DU-Net [13]	96.41	75.95	-	81.43	-
Patch-based Generative Adversarial Network (STARE) [49]	96.47	79.40	98.69	-	-
Adversarial Networks [54]	96.71	76.27	98.41	64.03	78.07
BSEResU-Net ([55]	95.43	74.97	98.42	-	-
MRA-Net[52]	97.63	84.2	98.7	-	84.2
Proposed Method	93,08	86,2	93,65	48,3	65,62

Table V is a segmentation results comparison of the proposed method with other studies on the STARE dataset. The highest accuracy and F1-score were obtained by Jiang et al. [52] but the sensitivity obtained was still lower than the sensitivity of the proposed method. The highest specificity was obtained by Li et al. [53], but the sensitivity obtained was still poor which was only 68.07%. The highest IoU was obtained by Jin et al. [13]. Unfortunately, the sensitivity was still below the sensitivity of other studies. In addition, this study did not measure specificity and F1-score. some other studies also has sensitivity below 80% namely Lv et al. [50], Ding et al. [46], Jin et al. , Isola et al. [54] but their IoU was higher than the IoU of the proposed method. The F1-score of the proposed method on STARE is still below 70%. This shows that the comparison between the prediction of blood vessels and the background is not balanced. The IoU on the stare dataset is also still low. It indicates that the method is still needed to improve to be able to separate between the background area and the area containing retinal blood vessels. The sensitivity of the method proposed in STARE is very good above 85% indicating the model has great performance in detecting blood vessels, especially for the thick retinal blood vessels.

Almost all of the studies in Table IV and Table V modified the U-Net architecture and proposed new architecture. The method proposed in this study does not modify the U-Net architecture but only modify the patching techniques in the training stage and testing stage to generate large data. However, the test results on the DRIVE dataset are excellent results of accuracy, specificity, and F1-score where the results obtained are above 90%. the sensitivity and IoU values are still below 90% but the proposed method is able to outperform several other studies. The results on the STARE dataset such as the accuracy, sensitivity, and specificity obtained are very good, but the F1-score and IoU in STARE is still needed to be improved. The results of the MCC and AUC area on the datasets also show that the proposed method is able to work well on unbalanced datasets where the number of background pixels is more than the number of retinal bool vessel pixels. The application of U-Net in this study is compared with the study of Lv et al. [50] which also used the conventional U-Net architecture. The results of the comparison of these two studies indicated that the patching technique in the proposed method significantly can improve the performance of conventional U-Net.

V. CONCLUSION

The application of the circular random patching technique and the ordered patching method to increase the training and testing data as well as obtain the required features is able to provide a great performance increase from the U-Net method. The patching technique provided input images with a smaller size but contained the features needed to retinal blood vessels segmentation. Although the U-Net architecture consisted of several layers, the application of this patching technique was able to help maximize the performance of U-Net even though the data being trained is a lot, namely by providing input with small but large amounts of data. In addition, the resulting performance parameters, namely accuracy, sensitivity, and specificity indicates that the proposed model provides excellent results in segmenting retinal blood vessels, especially for the DRIVE dataset. The ROC and AUC results also show that the model's performance is very good in segmenting the DRIVE or STARE dataset. The performance of the F1-score and IoU parameters for the DRIVE dataset are excellent, but in the STARE dataset, the F1-score and IoU values should be improved by various combinations of patching techniques and other CNN architectures.

REFERENCES

[1] Thayogo and A. Wibowo, "Weight-dropped long short term memory network for stock prediction with integrated historical and textual data," *IAENG International Journal of Computer Science*, vol. 47, no. 3, pp. 367–377, 2020.

[2] M. Badar, M. Haris, and A. Fatima, "Application of deep learning for retinal image analysis: A review," *Computer Science Review*, vol. 35, pp. 1-18, 2020.

[3] A. Desiani, Erwin, B. Suprihatin, S. Yahdin, A. I. Putri, and F. R. Husein, "Bi-path architecture of CNN segmentation and classification method for cervical cancer disorders based on pap-smear images," *IAENG International Journal of Computer Science*, vol. 48, no. 3, pp. 782–791, 2021.

[4] C. T. Nguyen, V. T. M. Khuong, H. T. Nguyen, and M. Nakagawa, "CNN based spatial classification features for clustering offline handwritten mathematical expressions," *Pattern Recognition Letters*, vol. 131, pp. 113–120, 2020.

[5] Z. Yoa, Z. Zhang, and L. Q. Xu, "Convolution neural network for retinal blood vessel segmentation," in *9th International Symposium on Computational Intellignece and Design, ISCID*, pp. 406–409, 2016.

[6] R. F. Rachmadi, I. K. Eddy Purnama, M. H. Purnomo, and M. Hariadi, "A systematic evaluation of shallow convolutional neural network on CIFAR dataset," *IAENG International Journal of Computer Science*, vol. 46, no. 2, pp. 365–376, 2019.

[7] O. Ronneberger, P. Fischer, and T. Brox, "U-Net: convolutional networks for biomedical image segmentation olaf," *MICCAI*, vol. 9351, no. 3, pp. 234–241, 2015.

[8] G. Du, X. Cao, J. Liang, X. Chen, and Y. Zhan, "Medical image segmentation based on U-Net: A review," *Journal Imaging Science Technology*, vol. 64, no. 2, pp. 1–12, 2020.

[9] S. Nurmaini *et al*.., "Automated detection of COVID-19 infected lesion on computed tomography images using faster-RCNNs," *Engineering Letters*, vol. 28, no. 4, pp. 1295–1301, 2020.

[10] T. A. Soomro, O. Hellwich, A. J. Afifi, M. Paul, J. Gao, and L. Zheng, "Strided U-Net model: Retinal vessels segmentation using dice loss," in *2018 International Conference on Digital Image Computing: Techniques and Applications, DICTA 2018*, pp. 1–8, 2018.

[11] L. Li, M. Verma, Y. Nakashima, H. Nagahara, and R. Kawasaki,

"IterNet: Retinal image segmentation utilizing structural redundancy in vessel networks," in *Proceedings - 2020 IEEE Winter Conference on Applications of Computer Vision, WACV 2020*, pp. 3645–3654, 2020.

[12] Z. Yan, X. Yang, and K. T. Cheng, "Joint segment-level and pixel-wise losses for deep learning based retinal vessel segmentation," *IEEE Transaction on Biomedical Engineering*, vol. 65, no. 9, pp. 1912–1923, 2018.

[13] Q. Jin, Z. Meng, T. D. Pham, Q. Chen, L. Wei, and R. Su, "DU-Net: A deformable network for retinal vessel segmentation," *Knowledge-Based System*, vol. 178, pp. 149–162, 2019.

[14] Z. Zhang, C. Wu, S. Coleman, and D. Kerr, "DENSE-INception U-Net for medical image segmentation," *Computer Methods Programs Biomedicine*, vol. 192, pp. 1–15, 2020.

[15] L. Bi, J. Kim, A. Kumar, M. Fulham, and D. Feng, "Stacked fully convolutional networks with multi-channel learning: application to medical image segmentation," *Visual Computer*, vol. 33, no. 6–8, pp. 1061–1071, 2017.

[16] J. Hamwood, D. Alonso-Caneiro, S. A. Read, S. J. Vincent, and M. J. Collins, "Effect of Patch Size and Network Architecture on a Convolutional Neural Network Approach for Automatic Segmentation of OCT Retinal Layers," *Biomedical Optics Express*, vol. 9, no. 7, pp. 3049–3066, 2018.

[17] T. B. Sekou, M. Hidane, J. Olivier, and H. Cardot, "From patch to image segmentation using fully convolutional networks-application to retinal images," *ArXiv*, pp. 1–21, 2019.

[18] Q. Zhang, G. Li, Y. Cao, and J. Han, "Multi-focus image fusion based on non-negative sparse representation and patch-level consistency rectification," *Pattern Recognition*, vol. 104, pp. 1–14, 2020.

[19] A. Nortje, W. Brink, H. A. Engelbrecht, and H. Kamper, "BINet: A binary inpainting network for deep patch-based image compression," *Signal Process Image Communication*, vol. 92, no. 116119, pp. 1–11, 2021.

[20] K. Trebing, T. Stańczyk, and S. Mehrkanoon, "SmaAt-U-Net: Precipitation nowcasting using a small attention-U-Net architecture," *Pattern Recognition Letter*, vol. 145, pp. 178–186, 2021.

[21] L. Rundo *et al*., "USE-Net: Incorporating squeeze-and-excitation blocks into U-Net for prostate zonal segmentation of multi-institutional MRI datasets," *Neurocomputing*, vol. 365, pp. 31–43, 2019.

[22] P. M. Samuel and T. Veeramalai, "VSSC Net: Vessel specific skip chain convolutional network for blood vessel segmentation," *Comput. Methods Programs Biomed.*, vol. 198, no. 105769, pp. 1–19, 2021.

[23] N. Sambyal, P. Saini, R. Syal, and V. Gupta, "Modified U-Net architecture for semantic segmentation of diabetic retinopathy images," *Biocybernetics and Biomedical Engineering*, vol. 40, no. 3, pp. 1094–1109, 2020.

[24] L. H. Shehab, O. M. Fahmy, S. M. Gasser, and M. S. El-Mahallawy, "An efficient brain tumor image segmentation based on deep residual networks (ResNets)," *Journal of King Saud University-Engineering Sciences*, vol. 33, no. 6, pp. 404–412, 2020.

[25] K. Kose *et al*., "Segmentation of cellular patterns in confocal images of melanocytic lesions in vivo via a multiscale encoder-decoder network (MED-Net)," *Medical Image Analysis*, vol. 67, no. 101841, pp. 1–12, 2021.

[26] R. Takahashi, T. Matsubara, and K. Uehara, "Data augmentation using random image cropping and patching for deep CNNs," *IEEE Trans. Circuits System Video Technology*, vol. 30, no. 9, pp. 2917–2931, 2020.

[27] Q. Guo, Y. Zhang, S. Qiu, and C. Zhang, "Accelerating patch-based low-rank image restoration using kd-forest and Lanczos approximation," *Information Science*, vol. 556, pp. 177–193, 2021.

[28] P. W. Hsieh and P. C. Shao, "Blind image deblurring based on the sparsity of patch minimum information," *Pattern Recognition*, vol. 109, pp. 1–17, 2021.

[29] J. Yu, D. Huang, and Z. Wei, "Unsupervised image segmentation via stacked denoising auto-encoder and hierarchical patch indexing," *Signal Processing*, vol. 143, pp. 346–353, 2018.

[30] D. Marín, A. Aquino, M. E. Gegúndez-Arias, and J. M. Bravo, "A new supervised method for blood vessel segmentation in retinal images by using gray-level and moment invariants-based features," *IEEE Transactions on Medical Imaging*, vol. 30, no. 1, pp. 146–158, 2011.

[31] Y. Liu and J. K. W. Yeoh, "Robust pixel-wise concrete crack segmentation and properties retrieval using image patches," *Automation in Construction*, vol. 123, no. 103535, pp. 1–17, 2021.

[32] Y. Tang, F. Ren, and W. Pedrycz, "Fuzzy C-Means clustering through SSIM and patch for image segmentation," *Applied Soft Computing Journal*, vol. 87, no. 105928, pp. 1–29, 2020.

[33] M. Shi, F. Zhang, S. Wang, C. Zhang, and X. Li, "Detail preserving image denoising with patch-based structure similarity via sparse representation and SVD," *Computer Vision and Image Understanding.*, vol. 206, no. 103173, pp. 1–11, 2021.

[34] X. Xiao, S. Lian, Z. Luo, and S. Li, "Weighted Res-U-Net for high-quality retina vessel segmentation," *Proc. - 9th Int. Conf. Inf. Technol. Med. Educ. ITME 2018*, pp. 327–331, 2018.

[35] M. I. Dillon, *Geometry Through History*. USA: Springer International Publishing AG, 2018.

[36] G. C. Cardarilli, L. Di Nunzio, R. Fazzolari, A. Nannarelli, M. Re, and S. Spano, "N-Dimensional approximation of euclidean distance," *IEEE Trans. Circuits Syst. II Express Briefs*, vol. 67, no. 3, pp. 565–569, 2020.

[37] Q. Li, W. Cai, X. Wang, Y. Zhou, D. D. Feng, and M. Chen, "Medical image classification with convolutional neural network," in *13th International Conference on Control Automation Robotics Vision (ICARCV)*, pp. 10–12, 2014.

[38] A. Desiani *et al*., "R-peak detection of beat segmentation and convolution neural network for arrhythmia classification," *Journal of Engineering Science Technology*, vol. 17, no. 2, pp. 1231–1246, 2022.

[39] T. A. Soomro *et al*., "Deep learning models for retinal blood vessels segmentation: a review," *IEEE Access*, vol. 7, pp. 71696–71717, 2019.

[40] S. Jadon, "A survey of loss functions for semantic segmentation," in *2020 IEEE Conference on Computational Intelligence in Bioinformatics and Computational Biology*, pp. 1–7, 2020.

[41] A. Desiani, S. Yahdin, A. Kartikasari, and I. Irmeilyana, "Handling the imbalanced data with missing value elimination smote in the classification of the relevance education background with graduates employment," *IAES International Journal of Artificial Intelligence*, vol. 10, no. 2, pp. 346–354, 2021.

[42] K. B. Park, S. H. Choi, and J. Y. Lee, "M-GAN: Retinal blood vessel segmentation by balancing losses through stacked deep fully convolutional networks," *IEEE Access*, vol. 8, pp. 146308–146322, 2020.

[43] Erwin, A. Noorfizir, M. N. Rachmatullah, and G. Sulong, "Hybrid multilevel thresholding-otsu and morphology operation for retinal blood vessel segmentation," *Engineering Letters*, vol. 28, no. 1, pp. 180–191, 2020.

[44] Erwin, Saparudin, M. Fachrurrozi, A. Wijaya, and M. N. Rachmatullah, "New optimization technique to extract facial features," *IAENG International Journal of Computer Science*, vol. 45, no. 4, pp. 523–530, 2018.

[45] C. Guo, M. Szemenyei, Y. Yi, W. Wang, B. Chen, and C. Fan, "SA-U-Net: Spatial attention U-Net for retinal vessel segmentation," in *2020 25th International Conference on Pattern Recognition (ICPR)*, pp. 1236–1242, 2021.

[46] H. Ding, X. Cui, L. Chen, and K. Zhao, "MRU-NET: A U-shaped network for retinal vessel segmentation," *Applied Science*, vol. 10, no. 19, pp. 1–18, 2020.

[47] O. Sule and S. Viriri, "Enhanced convolutional neural networks for segmentation of retinal blood vessel image," in *2020 Conference on Information Communications Technology and Society, ICTAS 2020 - Proceedings*, pp. 1–6, 2020.

[48] D. A. Dharmawan, D. Li, B. P. Ng, and S. Rahardja, "A new hybrid algorithm for retinal vessels segmentation on fundus images," *IEEE Access*, vol. 7, pp. 41885–41896, 2019.

[49] W. Abbas, M. H. Shakeel, N. Khurshid, and M. Taj, "Patch-based generative adversarial network towards retinal vessel segmentation," *Communications in Computer and Information Science*, vol. 1142, pp. 49–56, 2019.

[50] Y. Lv, H. Ma, J. Li, and S. Liu, "Attention guided U-Net with atrous convolution for accurate retinal vessels segmentation," *IEEE Access*, vol. 8, pp. 32826–32839, 2020.

[51] H. A. Leopold, J. Orchard, J. S. Zelek, and V. Lakshminarayanan, "PixelBNN: Augmenting the Pixel CNN with batch normalization and the presentation of a fast architecture for retinal vessel segmentation," *J. Imaging*, vol. 5, no. 2, 2019.

[52] Y. Jiang, H. Yao, C. Wu, and W. Liu, "A multi-scale residual attention network for retinal," *Symmetry (Basel).*, vol. 13, no. 24, pp. 1–16, 2021.

[53] X. Li, H. Chen, X. Qi, Q. Dou, C. W. Fu, and P. A. Heng, "H-DenseU-Net: Hybrid densely connected U-Net for liver and tumor segmentation from ct volumes," *IEEE Trans. Medical Imaging*, vol. 37, no. 12, pp. 2663–2674, 2018.

[54] P. Isola, J.-Y. Zhu, T. Zhou, and A. A. Efros, "Image-to-image translation with conditional adversarial networks," in *2017 IEEE Conference on Computer Vision and Pattern Recognition (CVPR)*, pp. 5967–5976, 2017.

[55] D. Li and S. Rahardja, "BSEResU-Net: An attention-based before-activation residual U-Net for retinal vessel segmentation," *Computer Methods Programs Biomed.*, vol. 205, no. 106070, pp. 1-11, 2021.

Anita Desiani was born in Palembang, Indonesia, in 1977. In 2020, She is currently working on a project for her Doctoral Program at Mathematics and Natural Science Faculty, Universitas Sriwijaya. She received mathematics bachelor from Universitas Sriwijaya in 2000, and magister degree in Computer Science from Universitas Gadjah Mada in 2003. In the same year, she joined as lecturer at Mathematics Department in Universitas Sriwijaya until now. Her current research interests include in the field of data mining, image processing, pattern recognition and computer vision and artificial intelligent.

Erwin was born in Palembang, Indonesia, in 1971. He received his Bachelor of Mathematics from Universitas Sriwijaya, Indonesia, in 1994, and an M.Sc. degree in Actuarial from the Bandung Institute of Technology (ITB), Bandung, Indonesia, in 2002. In 1 994, he joined Universitas Sriwijaya, as a Lecturer since December 2006, he has been with the Department of Informatics, Universitas Sriwijaya, where he is an Associate Professor in 2011. Since 2012, he has been with the Department of Computer Engineering, Universitas Sriwijaya. Then, in 2019, he received his Doctorate in Engineering, Faculty of Engineering, Universitas Sriwijaya. His current research interests include image processing, and computer vision. Dr. Erwin, S.Si, M.Si is a member of IAENG and IEEE.

Bambang Suprihatin was born in Salatiga, Indonesia, in 1971. He received his Bachelor of Mathematics from Universitas Sriwijaya, Indonesia, in 1994, and an M.Sc. degree in Mathematics from the Bandung Institute of Technology (ITB), Bandung, Indonesia, in 2002. In 1994, he joined Universitas Sriwijaya, as a Lecturer. He was Associate Professor in 2011. Since 2012, he received his Doctorate in Mathematics, Universitas Gadjah Mada (UGM) in 2016. His current research interests are statistics and modeling.

Ermatita was born in Lahat, September 1967. She received mathematics bachelor from Universitas Lampung in 1991, and magister degree in Computer Science from Universitas Indonesia in 1999 and Doktor Degree in Computer Science from Universitas Gadjah Mada in 2013. She currently working on Universitas Sriwijaya start since 2006. She is an Associate Professor in 2013. Her research interets are artificial intelligent, data mining. Machine learning and Information System.

Fathur Rachman Husein was born in Palembang, 1988, Indonesia He is currently working on a project for his undergraduate degree at Mathematics Department, science and nature Faculty, Universitas Sriwijaya. In 2018, he joined the Laboratory of Computation Mathematics and Natural Science Faculty, Universitas Sriwijaya as Assistant Lecturer. His current research interests include in the field of data structure, image processing, pattern recognition and computer vision, data mining and artificial intelligent.

Yogi Wahyudi was born in Palembang, March 2000.He is currently working on a project for his undergraduate degree at Mathematics Department, science and nature Faculty, Universitas Sriwijaya. In 2018, he joined the Laboratory of Computation Mathematics and Natural Science Faculty, Universitas Sriwijaya as Assistant Lecturer. His current research includes in the field of image processing, pattern recognition and computer vision, data mining and artificial intelligent.

A Novelty Patching of Circular Random and Ordered Techniques on Retinal Image to Improve CNN U-Net Performance

ORIGINALITY REPORT

14%	9%	12%	2%
SIMILARITY INDEX	INTERNET SOURCES	PUBLICATIONS	STUDENT PAPERS

MATCH ALL SOURCES (ONLY SELECTED SOURCE PRINTED)

1%

★ Lecture Notes in Computer Science, 2010.

Publication

Exclude quotes	On	Exclude matches	Off
Exclude bibliography	On		